

# DESIGN OF POLARIZATION-PRESERVING CIRCULAR WAVEGUIDE FILTERS WITH ATTENUATION POLES

Smain Amari<sup>1</sup> and Jens Bornemann<sup>2</sup>

<sup>1</sup> Department of Electrical and Computer Engineering  
Royal Military College  
Kingston, Ont. K7K 7B4, Canada

<sup>2</sup> Department of Electrical and Computer Engineering  
University of Victoria  
Victoria, B.C. V8W 3P6, Canada

Received 22 June 2001

**ABSTRACT:** Bandpass filters in circular waveguide technology are designed to have enhanced stopband responses. Highly dispersive coupling sections are introduced to replace regular circular irises. The resulting direct-coupled resonator bandpass filters have the advantage of preserving the polarization of the incident excitation while providing sharp cutoff skirts. Attenuation poles at finite frequencies are generated on either side of the passband by using radial stubs, which also perform the role of inverters. In contrast to the pole-extraction technique, or the classical technique of using stubs for the sole purpose of pole generation, the zero-generating elements act as inverters, and are not necessarily the first elements at the input and/or output. A simple approximate design technique which provides adequate starting values for optimization-based design is also introduced. Design examples are presented to show the validity of the approach and the performance of these filters. © 2001 John Wiley & Sons, Inc. *Microwave Opt Technol Lett* 31: 334–336, 2001.

**Key words:** circular waveguide filters; filters; polarization

## I. INTRODUCTION

The design of elliptic and pseudoelliptic bandpass filters in circular waveguides is usually based on the introduction of cross coupling between the resonators, e.g., [1, 2]. In circular waveguide technology, the cross coupling is achieved, e.g., by utilizing the two polarizations of the TE<sub>11</sub> mode and coupling sections, such as rectangular, elliptic, or cross-shaped irises, and coupling screws, e.g., [1]. A third alternative, especially for transmission zeros relatively far from the passband, consists of properly placing the output with respect to the input [2]. For all of these designs, the excitations are required to be aligned with two prescribed orthogonal directions for the filter to perform properly. They cannot be used in systems with circular polarization. These systems typically imply all-iris circular waveguide filters which, in their standard form, are incapable of generating attenuation poles (transmission zeros) in the vicinity of the passband.

In this paper, we propose to use strongly dispersive coupling in direct-coupled TE<sub>11</sub>-mode resonator filters to generate finite transmission zeros. The design technique is based on circular sections of larger radii than the main waveguide, i.e., radial stubs, which preserve the polarization of the incident wave. Moreover, this technique allows the zero-generating elements to replace practically any coupling section of the filter. As such, the designs are noticeably different from what is generally known as the extracted pole technique.

## II. THEORY

The first step in the design is to perform a filter synthesis for directly coupled resonators, e.g., [2, 3]. The so-obtained inverter prototype values are realized by an iterative algorithm

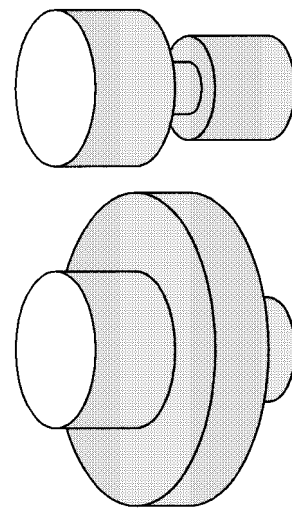


**Figure 1** Inverters between two circular waveguides: low-dispersive circular iris (top), highly dispersive radial stub (bottom)

which matches the fundamental-mode scattering parameters of a circular iris (Fig. 1, top) to the prototype inverter. Although the following formulas have been developed for inductive coupling in rectangular waveguides, they have been successfully used by the authors in the design of circular iris filters for many years:

$$jX_{s1} = \frac{[1 + S_{11}][1 - S_{22}] + S_{21}^2 - 2S_{21}}{[1 - S_{11}][1 - S_{22}] - S_{21}^2} \quad (1)$$

$$jX_{s2} = \frac{[1 - S_{11}][1 + S_{22}] + S_{21}^2 - 2S_{21}}{[1 - S_{11}][1 - S_{22}] - S_{21}^2} \quad (2)$$

$$jX_p = \frac{2S_{21}}{[1 - S_{11}][1 - S_{22}] - S_{21}^2} \quad (3)$$

$$\begin{bmatrix} \phi_1 \\ \phi_2 \end{bmatrix} = -\arctan \left\{ \frac{X_{s1} + X_{s2} + 2X_p}{1 - X_{s1}X_{s2} - X_p(X_{s1} + X_{s2})} \right\} \mp \arctan \left\{ \frac{X_{s1} - X_{s2}}{1 + X_{s1}X_{s2} + X_p(X_{s1} + X_{s2})} \right\} \quad (4)$$

$$K = \sqrt{\left| \frac{1 + \Gamma \exp(-j\phi_1)}{1 - \Gamma \exp(-j\phi_1)} \right|} \quad (5)$$

$$\Gamma = \frac{(jX_{s1} + jX_p - 1)(jX_{s1} + jX_p + 1) + X_p^2}{(jX_{s1} + jX_p + 1)(jX_{s1} + jX_p + 1) + X_p^2} \quad (6)$$

$X_s$  and  $X_p$  are the series and shunt reactances of the equivalent T-circuit with transmission lines of electrical lengths  $\phi_1$  and  $\phi_2$  attached at the input and output, respectively. A circular waveguide iris filter designed in this fashion cannot generate finite attenuation poles without “overmoding” the resonators.

In order to introduce these poles, we change some irises into stubs (Fig. 1, bottom). By adjusting the width and radius of the stub, it is possible to introduce finite attenuation poles on either side of the passband. This is demonstrated in Figure 2(a) (solid line). The zeros of the normalized inverter produce attenuation poles in the overall filter response. Note that this is not possible with the circular iris (dashed line).

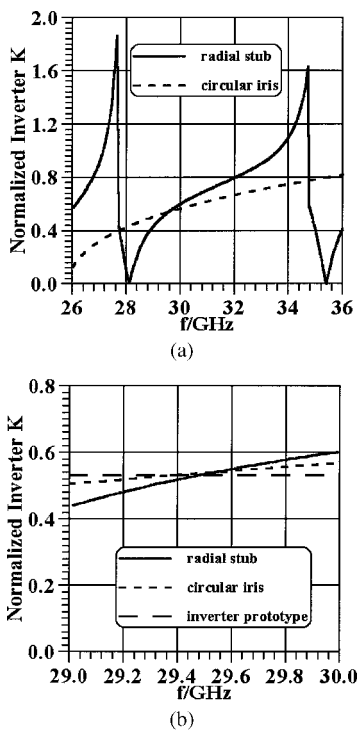


**Figure 2** Inverter behavior of low-dispersive circular iris and highly dispersive radial stub. (a) Wideband. (b) Narrowband

However, the role of a radial stub is not limited to the introduction of the poles. It is also used to provide the correct prototype inverter value in the passband [Fig. 2(b)]. Although the frequency variation of the radial stub (solid line) over the passband between 29–30 GHz is slightly larger than that of the circular iris (short dashed line), the maximum relative deviation from the inverter prototype target value (long dashed line) is on the order of 15%, which is acceptable in practical filter designs.

The initial design of a radial stub uses (1)–(6) for calculating the inverter value for given dimensions and the coupled-integral-equation technique (CIET), e.g., [4], to determine the scattering parameters. The next step consists of adjusting the stub dimensions to satisfy the two rather conflicting conditions of maintaining a constant inverter value over the passband of the filter and yielding transmission zeros at the desired frequencies. Obviously, the first condition cannot be satisfied exactly. A more realistic request is to require the coupling section to achieve the desired inverter value only at the center frequency of the filter as, e.g., in rectangular  $TE_{10}$ -mode waveguide filters [5]. However, it was realized that such an approach does not work well for the  $TE_{11}$  mode in a circular waveguide. Therefore, the following criterion was used. The deviation between the desired inverter value and the value obtained from the coupling section is minimized over the passband of the filter using a sufficient number of frequency points. In other words, the approximate dimensions of the zero-generating coupling section are determined from the minimization of the cost function:

$$F_{\text{cost}} = \sum_i [K_{\text{prototype}} - K_{\text{stub}}(\omega_{pi})]^2 + |S_{21}(\omega_{z1})|^2 + |S_{21}(\omega_{z2})|^2 \quad (7)$$

where  $\omega_{z1}$ ,  $\omega_{z2}$  are the locations of the transmission zeros, and  $\omega_{pi}$  are frequencies in the passband of the filter. Note that the number of transmission zeros in practical applications is usually small. Therefore, only one or two radial stubs are required, while the remaining coupling sections can be realized as traditional circular irises. After synthesis of all radial stubs and circular irises, the entire filter structure is optimized, e.g., [6], for passband return loss while maintaining the positions of attenuation poles.

### III. RESULTS

Figure 3 shows a design example for a six-pole filter with a single transmission zero in the upper stopband. The zero-generating radial stubs are chosen as the second coupling sections from the input and output. Since each stub in this symmetric structure generates its own zero, the transmission zero shown in Figure 3 is of second order. The long dotted line shows the typical response of a standard circular iris filter. After replacing the two irises with radial stubs using the procedure outlined above, an approximate design is obtained (short dashed line). Although the approximate design does not achieve the desired return loss, it gives a well-defined passband and the transmission zero at the specified frequency. Most importantly, it provides a good starting point for any optimization routine. The response of the optimized filter is shown as the solid line in Figure 3. Compared with the standard circular iris filter, the sharper cutoff skirt achieved through the second-order transmission zero is substantial.

The second design example is a five-pole filter with a single transmission zero to the left of the passband and two in the upper stopband. The finalized asymmetric design and its response are shown in Figure 4. An inband return loss of 26 dB is achieved, and the presence of the transmission zeros is evident. The CIET results are validated by comparison with an independently developed mode-matching technique (MMT) code (dashed line).

The final example is also a five-pole filter, but with one transmission zero on each side of the passband. The in-band return loss is 30 dB. Figure 5 shows the presence of the optimized filter. All of the specifications are met, in particular, the presence of the two transmission zeros. Since the structure is symmetric, and each radial stub generates its own zeros, the transmission zeros of the assembled filter are of

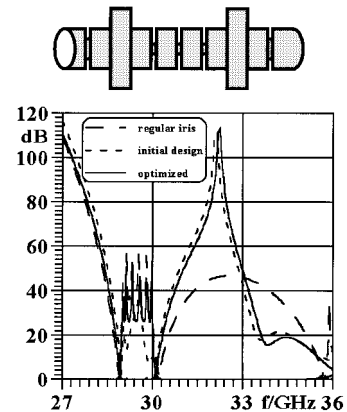


**Figure 3** Performance of a symmetric six-pole filter with one transmission zero in upper stopband. Second and sixth irises are converted to dispersive inverters

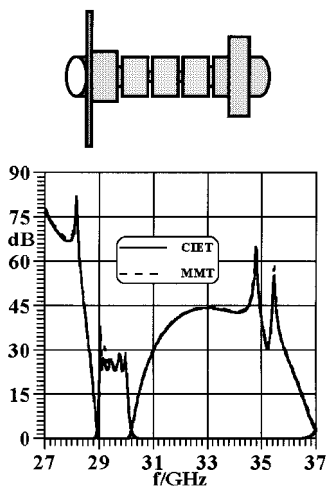


**Figure 4** Performance of an asymmetric five-pole filter with two transmission zeros in upper stopband and one transmission zero in lower stopband. First and last irises are converted to dispersive inverters. Comparison with the mode-matching technique (MMT)

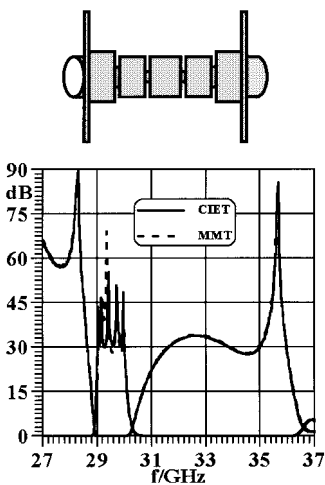


**Figure 5** Performance of a symmetric five-pole filter with one transmission zero in upper stopband and one transmission zero in lower stopband. First and last irises are converted to dispersive inverters. Comparison with the mode-matching technique (MMT)

second order. The second-order zeros are more effective in pushing the insertion loss further up (in the stopband) and “widening” the transmission zeros, thereby increasing the cutoff rate.

#### IV. CONCLUSIONS

Circular waveguide filters with polarization-preserving capability can be designed to accommodate specifications for attenuation poles (transmission zeros) close to and at either side of the passband. The concept of replacing circular irises (and not necessarily the ones closest to the input and output) by strongly dispersive radial stubs allows the application of an approximate design technique which provides an adequate response for further optimization. Three example filter designs for a 29–30 GHz passband and comparisons between the CIET and the MMT validate the presented approach.

#### REFERENCES

1. J. Uher, J. Bornemann, and U. Rosenberg, Waveguide components for antenna feed systems: Theory and CAD, Artech House, Norwood, MA, 1993.
2. G.L. Matthaei, L. Young, and E.M.T. Jones, Microwave filters, impedance matching networks and coupling structures, Artech House, Dedham, MA, 1980.
3. S.B. Cohn, Direct-coupled-resonator filters, Proc IRE 45 (1957), 187–196.
4. S. Amari, J. Bornemann, R. Vahldieck, and P. Leuchtman, Spectrum of corrugated and periodically loaded waveguides from classical matrix eigenvalues, IEEE Trans Microwave Theory Tech 48 (2000), 453–460.
5. S. Amari and J. Bornemann, Using frequency-dependent coupling to generate attenuation poles in direct coupled resonator filters, IEEE Microwave Guided Wave Lett 9 (1999), 404–406.
6. K. Madsen, O. Nielsen, H. Schaer-Jacobsen, and L. Thrane, Efficient minimax design of networks without using derivatives, IEEE Trans Microwave Theory Tech MTT-23 (1975), 803–809.

© 2001 John Wiley & Sons, Inc.

## OPTICAL CODE-DIVISION SWITCHING NETWORK BASED ON SIMULTANEOUS CAPACITY PRIME CODE

Yang-Han Lee,<sup>1</sup> Rong-Hou Wu,<sup>1</sup> and Fun Yu<sup>1</sup>

<sup>1</sup> Department of Electrical Engineering  
Tamkang University  
Tamsui, Taipei Hsien, Taiwan 251, R.O.C.

Received 16 June 2001

**ABSTRACT:** In this paper, a novel optical switch OCDSN (optical code-division switching network) using the simultaneous capacity of the prime code is proposed. Selecting the prime code in accordance with transmission routing forms the basis of this three-layer network architecture. This network code switching provides one-to-one, multicast, and broadcast characteristics. The optimal connection methods and modularized design are proposed. From mathematical analysis, we see that the optical nodes of the OCDSN are less complex than Omega's. And the optical nodes of the modularized  $P_3$  OCDSN are almost half in number as compared to the  $P_3$  OCDSNs under the same input port conditions. © 2001 John Wiley & Sons, Inc. Microwave Opt Technol Lett 31: 336–340, 2001.

**Key words:** optical code-division switching network; prime code

#### I. INTRODUCTION

Fiber-optical communications have developed very quickly after the first low-loss fibers were proposed in 1970. Since 1984, fibers have crisscrossed much of the United States and many other countries to deliver telephone messages between major exchanges. In previous research, spatial-domain switching [1–2], wavelength-domain switching [3], and time-domain switching techniques [4] were used. However, there are defects in each of these techniques. First, the defect of the spatial-domain switching technique is the increasing number of nodes and layers with input end numbers. Then, the defect of the wavelength-domain switching technique is the difference of the path loss for every wavelength. This makes the routing control become more complicated, and limits the numbers of wavelengths. Finally, the defect of the time-

Contract grant sponsor: National Science Council, Taipei, Taiwan, R.O.C. Contract grant number: NSC 89-2215-E-032-006